中國機械工程學刊第四十三卷第一期第 37~46 頁(民國一百一十一年)
Journal of the Chinese Society of Mechanical Engineers, Vol.43, No.1, pp 37~46 (2022)

Enhanced Tribological Property of Mechanical Seal in Water Environment by Nanosecond Laser Surface Texturing

Wei-Gang Zhao *, Qi Liu**, Heng-Di Yuan**, Yi-Hong Li** and Guang-Neng Dong***

Keywords: mechanical seal, laser texturing, tribological property, turbopump.

ABSTRACT

Mechanical seal used in turbopump of liquid rocket engine always underwent sever wear and friction-induced vibration in the running stage. Here, an effective circle-shaped texture dimple was proposed to be manufactured on S07 steel surface, and its surface morphology, mechanical property and tribological performance were investigated systematically. To simulate the low viscosity of sealed liquid in the turbopump, the tribology test was conducted in water environment. Textures with different area ratios were manufactured and the experimental results showed that the texture whose area ratio is 10% (T10) is the most efficient. More tribological experiments under different temperatures, frequencies and loads were conducted, and the results showed that the T10 textured surface can decrease the friction coefficient, enhance the stability of friction behaviors and reduce wear rate. Moreover, the tribological mechanism of the texture was explored and analyzed according to the SEM and EDS of the wear tracks. The soft Cu/graphene composite can fill the texture dimples and form a tribo-film on the surface, which helps to reduction of friction and wear.

INTRODUCTION

The turbopump system has been extensively used in aerospace to feed high-pressure propellant such as liquid oxygen to the combustion chamber of liquid rocket engine due to its lightweight characteristic and compact structure (Wang et al., 2012). In practical applications, the working performance of turbopump was greatly affected by its sealing effect, and the undesirable medium leakage might cause serious economic loss and safety problems. As is known, the liquid rocket engine works in harsh conditions, such as the low temperature of cryogenic propellants, heavy load and high speed, which hence put forward high requirement for the reliability and sealing performance of turbopump (Palerm et al., 2015). Thus, improving the sealing performance is vital in enhancing the working performance of turbopump as well as the liquid rocket engine.

Nowadays, mechanical seal has been widely used in various mechanical systems including the turbopump system due to its superior sealing performance, simple structure and relatively low cost. The working reliability of the mechanical seal was mainly affected by its friction and wear properties. However, the sealed medium could not provide effective lubrication to the seal pair due to its low viscosity (Zhang et al., 2017). Thus, the mechanical seal used in aerospace usually employed soft-hard pattern to decrease friction and wear, such as steel and copper/graphite composite (Johnson et al., 2013; Bullen, 2014; Lu et al., 2018). However, the seal pair still faced sever wear and friction-induced vibration in the operating period, especially the start-up stage, during which the seal pair was in poor lubrication regime such as mixed or boundary regime (Zhang et al., 2011). There is no doubt that the sever wear and undesirable vibration would negatively affect its working reliability, service time and sealing performance, which could bring about numerous economic, environmental and safety issues.

For the past decades, many efforts have been done to improve the tribological performance of turbopump system, including material modification and surface treatment, such as doping coatings and creating texture patterns (Zhang et al., 2010; Wang et al.,

Paper Received June, 2020. Revised February, 2021. Accepted March, 2021. Author for Correspondence: Qi Liu

* *Graduate Student, School of Astronautics, Northwestern Polytechnical University, Xi'an 710049, PRC.*

** *Graduate Student, Key Laboratory of Education Ministry for Modern Design and Rotor-Bearing System, Xi'an Jiaotong University, Xi'an, 710049, PRC.*

*** *Professor, Key Laboratory of Education Ministry for Modern Design and Rotor-Bearing System, Xi'an Jiaotong University, Xi'an, 710049, PRC.*

2012; Etsion et al., 2002). However, the inadequate adhesion strength of coatings to underlying substrate limits its use in heavy-load applications (Ma et al., 2016). Compared with doping coatings, creating texture pattern directly on material surface is simple and commercial, which has great potentials in future applications. It has been reported by Refs. (Qiu et al., 2011; Bai et al., 2010; Brunetière et al., 2012; Li et al., 2018) that creating texture pattern on material surface was effective in decreasing friction and wear, which improved tribological property through a complex mechanism. On the one hand, texture pattern manufactured on material surface could act as traps for abrasive particles and debris, which was beneficial to eliminating the abrasive wear and plough effect. On the other hand, the texture pattern could also be effective in reserving liquid lubricants and inducing local hydrodynamic lubricating effect, which contributed to the enhancement of the load bearing capability and the lubricating condition. Furthermore, the manufactured texture pattern could also decrease the actual contacting area and hence decrease friction force and friction coefficient.

Up to now, many techniques have been successfully used to manufacture texture pattern on material surface, such as reactive ion etching (Wang et al., 2003), electrochemical methods (Silva et al., 2017), CNC machining (He et al., 2018) and laser texturing machining (Zhang et al., 2016), etc. Among these techniques, laser texturing treatment is more attractive due to its commercial, environmentally- clean and high-efficiency characteristics. Our group (Zhang et al., 2014, 2016; Li et al., 2020) has also done a lot work concerning the lubricating effectiveness of texture pattern through numerical analysis and experimental tests, and the results showed that manufacturing texture pattern on material surface was effective in improving its tribological performance in mixed or starved lubrication regime. Thus, it was promising and rational to manufacture texture pattern to improve its comprehensive tribological performance.

Many researches have done works concerning the effect of textured surface on the tribological properties of friction pairs, but most researches were conducted with normal steel, which has no reference for the lubrication of the seal parts of turbopump system in aerospace. S07 steel is one of the materials often used in aerospace, which has good mechanical properties, such as high strength, high toughness and corrosion resistance.

In this paper, three types of circle-shaped texture dimples were manufactured on the S07 steel surface by nanosecond laser machine. The surface morphology and mechanical property were analyzed by SEM, EDS and 3D laser confocal microscope. In order to simulate the low-viscosity liquid atmosphere of mechanical seal used in liquid rocket engine (Zhang et al., 2017), the tribological test was performed in water environment by a pin-on-disk tribometer under different temperatures, frequencies and loads. Furthermore, the morphology of the wear tracks was investigated, and lubricating mechanisms were also discussed systematically.

EXPERIMENT

Manufacture of texture patterns

Commercially available S07 steel disk (diameter=40 mm, depth=5 mm) was used as the substrate for laser texturing treatment. Prior to laser treatment, the steel surface was polished by 400#, 800# and 1200# sandpaper successively so that the surface roughness (Ra) was no more than 30 nm. Then, the steel surface was cleaned by ethanol and subsequently distilled water with an ultrasonic cleaning machine. After the cleaned steel was dried in an electrical oven, the steel surface was subject to laser texturing treatment. As seen in Figure 1, the circle-shaped texture patterns (radius, R=100 μm) were created on steel surface by nanosecond laser fiber machine (QC-F20) with laser wavelength of 1064 nm at ambient atmosphere. The area ratios were set as 5% (T5), 10% (T10) and 20% (T20) and the corresponding parameters are presented in Table 1. During the texture machining process, the laser scanning speed, scanning times and output power were set as 500 mm/s, 4 times and 16 W, respectively. Then, the textured steel surface was slightly polished by 1200# sandpaper to remove the laser ablation-induced burrs distributed on the edge of texture pattern. The polished textured steel was then ultrasonically cleaned in ethanol and then dried thoroughly for further characterization.

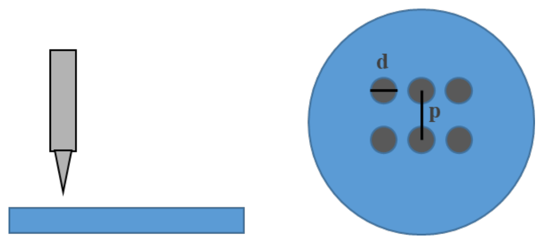

Fig. 1. The scheme diagram of manufacturing texture pattern by nanosecond laser machine.

Table 1. The design parameters of three textures.

Specimen	Texture pattern	Diameter, d (μm)	Texture pitch, p (μm)	Area ratio
T5	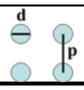	100	400	5%
T10		100	280	10%
T20		100	200	20%

Surface characterization

The surface morphology and corresponding element composition of S07 steel surface before and after laser texturing treatment were characterized by optical microscope (CX40M, China), SEM (SU-8010, HITACHI) and EDS (Oxford INCA Energy, UK). The three-dimensional morphologies of were analyzed by

3D laser confocal microscope (OLS4000, OLYMPUS, Japan).

Tribological property

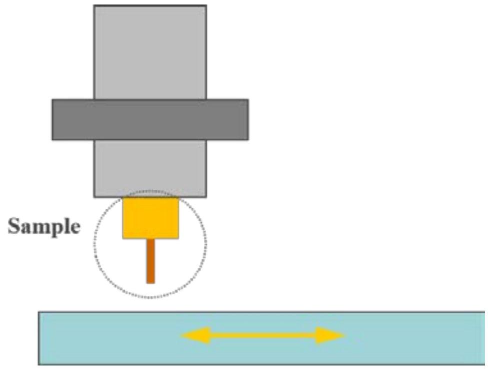

Fig. 2. The scheme diagram of the pin-on-disk tribological experiments.

The tribological property of the S07 steel disk against copper/graphite composite pin in water environment was tested through CETR tribometer (Corporation Ltd., USA) with the loads of 3-20 N, 30-100 N and frequencies of 1-5 Hz. The stroke was 6 mm, and the diameter of the pin is 3 mm (Figure 2). The pin was chamfered to avoid the effect of attack angle. After the friction test, the wear scar on disk and pin was analyzed by SEM, EDS and laser confocal microscope (LSM700, Germany). Furthermore, the specific wear rate of disk was calculated by the following question:

$$Ws = \frac{Al}{FL}, \tag{1}$$

where A was the cross-sectional area of wear scar, l was the amplitude of reciprocating motion, F was the applied load and L corresponded to the total sliding length. Each test was conducted three times, and the average data was presented.

Table 2. The detailed experiment conditions.

Item	Value	
Test1	Untextured, T5, T10, T20	10N, 2Hz
Test2	Untextured, T10	20ºC, 10N, 2Hz; 70ºC, 10N, 2Hz
Test3	T10	30-100N, 2Hz
Test4	T10	10N, 1-5Hz
Test5	T10	3-20N, 2Hz

ERESULT AND DISCUSSION

Surface morphology and composition

The morphology of the untextured surface and the textures after laser processing are presented in Figure 3. The distance between adjacent texture dimples of T5, T10 and T20 are 400, 280 and 200 μm. It can be seen clearly that there are some burrs around the circular dimples. This was because during the laser surface texturing process, part of the substrates was oxidized and splashed while some materials were accumulated around the circular dimple.

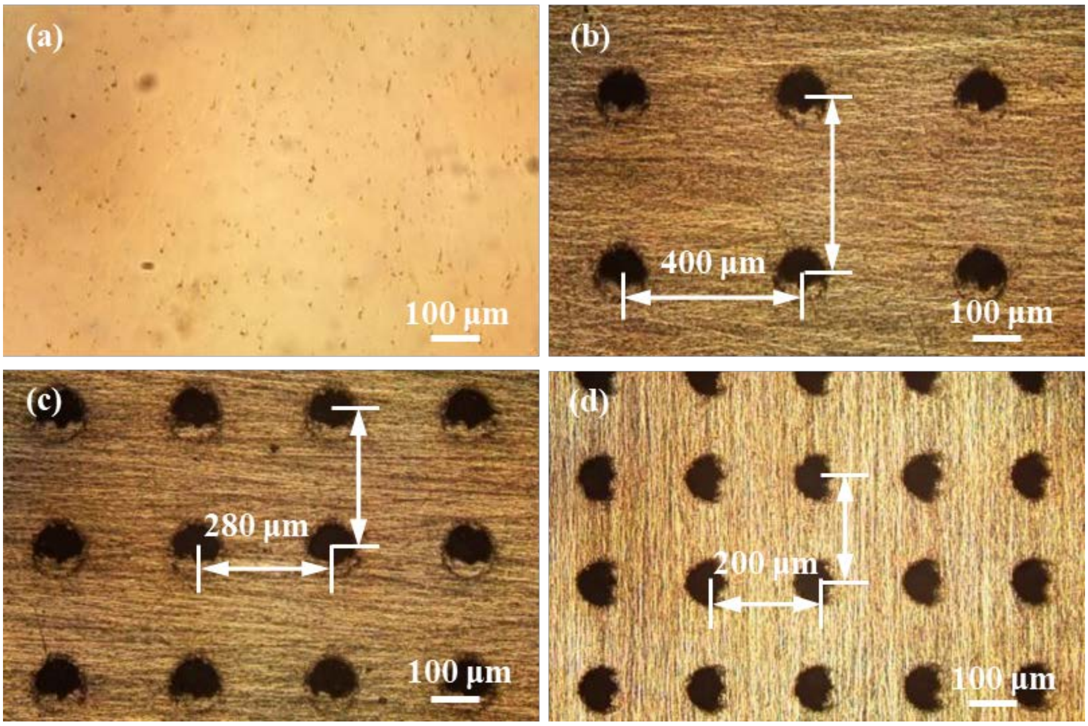

Fig. 3. The surface morphology of the (a) original disk surface and the laser textured surfaces of different area ratio: (b) T5, (c) T10, (d) T20.

The surface morphology and element composition of S07 steel before and after texturing treatment were illustrated in Figure 4. As shown in Fig. 4a, the surface of untextured steel was relatively smooth, though same shallow grooves could be identified due to the previous polishing process. Then the element composition was analyzed by EDS, as shown in Fig. 4b. The concentration of C, O, Cr, Mn, Fe and Ni elements were 24.86 at.%, 3.26 at.%, 12.47at.%, 1.53at.%, 52.97 at.% and 4.91 at.%, respectively.

Fig. 4c illustrated the surface morphology of laser textured S07 steel. It could be seen that ideal circle-shaped texture dimple with diameter of about 100 μm was successfully created on the steel surface. As shown in Fig. 4d, the EDS spectrum of textured steel was similar to that of untextured S07 steel. As for the element composition, it could be found the content of O element increased sharply to 15.42 at.% after the laser texturing process, while the content of Mn and Fe elements decreased dramatically to 0.56 at.% and 39.67 at.% respectively. Furthermore, the concentration of C element also increased slightly to 31.78 at.%. The increase of O element content indicated that the steel surface had been oxidized during the laser texturing process. It is known that the laser machine builds texture pattern on material surface via laser ablation and evaporation (Kusinski et al., 2012). Therefore, the reaction of steel surface with air might be accelerated, which hence changed its chemical composition.

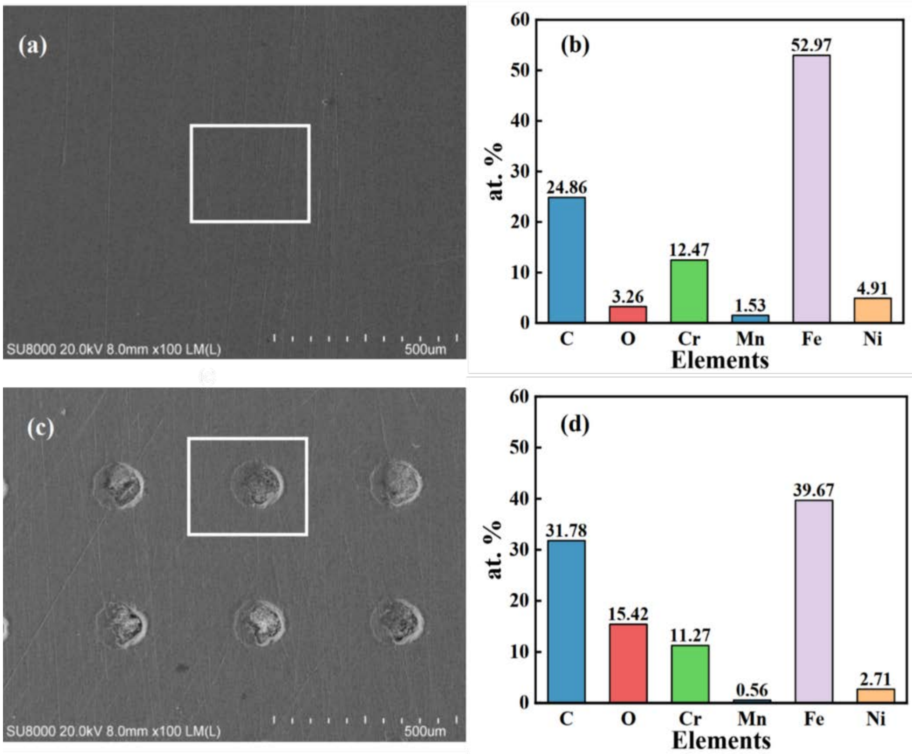

Fig. 4. The surface morphology and EDS spectra of (a-b) S07 steel and (c-d) laser textured S07 steel T10.

The surface, cross-section and three-dimensional morphologies of textured dimple on S07 steel are presented in Figure 5. As seen in Fig. 5a, circle-shaped texture dimple was manufactured on S07 steel through laser ablation process. The cross-section and three-dimensional morphologies of textured steel were also obtained through the analysis of 3D laser confocal microscope, which are presented in Fig. 5b and Fig. 5c. As shown in Fig. 5b, the diameter of circle-shaped texture dimple was about 100 μm, and the corresponding depth was around 26 μm. As illustrated in Fig. 5c, the 3D morphology of textured steel shows circle-shaped dimple with relatively flat upper surface and bottom surface. Thus, it could be concluded that the circle-shaped texture dimple with diameter of 100 μm and depth of 26 μm had be successfully built on the S07 steel surface by nanosecond laser fiber machine, and the texture dimple showed relatively flat upper surface.

Tribological property of the textured surface

The average friction coefficients and friction curves of untextured S07 surface and textured surfaces with different area ratios after tribological experiments are shown in Figure 6. Fig. 6a shows that the textured surfaces have good effect on friction decrease. Compared with the untextured surface, T5, T10 and T20 can decrease the average friction coefficient by 10.4%, 12.5% and 6.25% respectively. Among the three textured surface, T10 can mostly decrease the friction coefficient. As for the corresponding friction coefficient curves in Fig. 6b, the friction coefficient curves of the untextured disk and T5 fluctuate greatly while these of T10 and T20 are more stable. The above results show that the textured surface can efficiently decrease the friction coefficient, and the T10 texture is the most efficient.

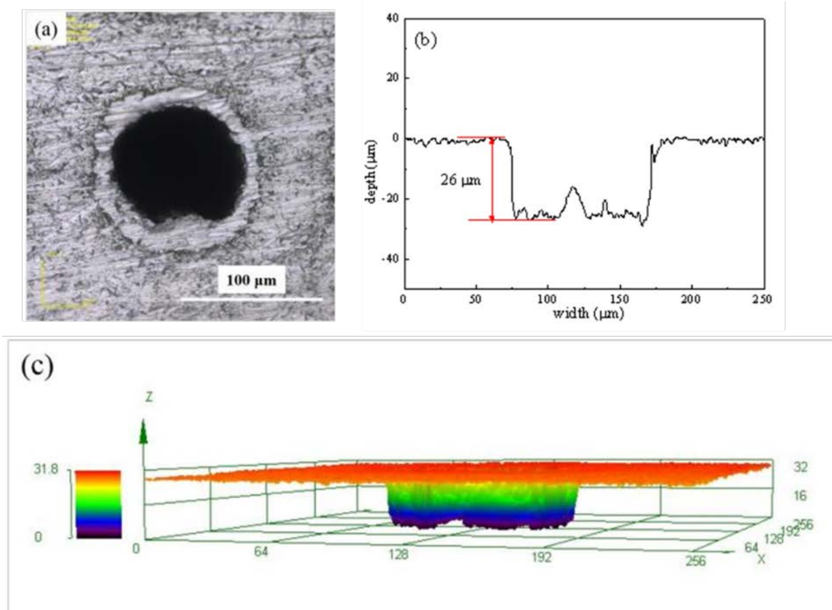

Fig. 5. The images of (a) the surface, (b) cross-section and (c) three-dimensional morphologies of texture dimple (T10) manufactured on steel surface.

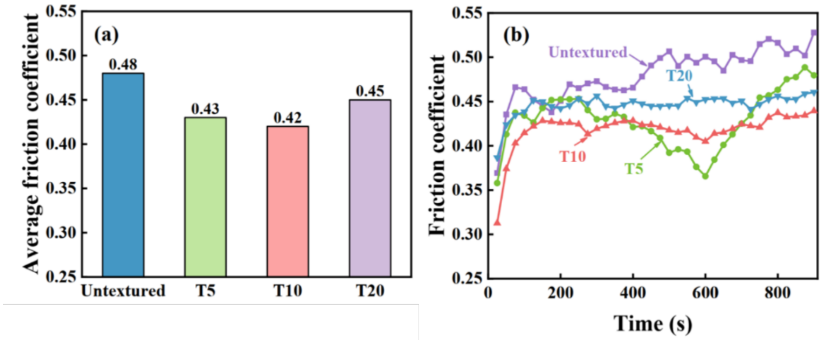

Fig. 6. The (a) average friction coefficients of the untextured surface, T5, T10 and T20 and (b) the corresponding friction coefficient curves under experimental conditions of 10N and 2Hz

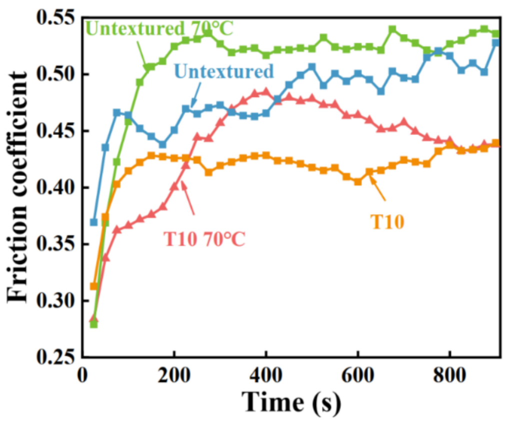

Fig. 7. The friction coefficient curves of the untextured surface and T10 under different temperatures

More experiments under different temperatures of untextured and T10 textured surfaces were conducted. The friction coefficient curves of the untextured and T10 textured disks under room temperature and 70 ºC are displayed in Figure 7. It is obviously that both untextured and T10 textured surface get larger friction coefficients under high temperature. However, the friction curves of T10 textured surface under room temperature and 70 ºC were lower that these of untextured surface, which showed that the T10 textured surface can reduce friction coefficient not only under room temperature but also high temperature, further proving the effectiveness of T10 textured surface in friction reduction.

Due to the softer material properties of copper/graphite composite than S07 steel disk, wear is not easy to form on the surface of the steel disk, which makes it difficult to detect and calculate the wear rate. Therefore, the experimental loads were increased to study and compare the anti-wear properties of untextured surface and T10 texture.

The average friction coefficient, corresponding friction curves and wear rate of the untextured and T10 textured steel are presented in Figure 8. The average friction coefficients of the untextured and T10 textured surface is displayed in Fig. 8a. The results show that as the loads increase, the average friction coefficient of the untextured steel decrease while these of the T10 texture increase.

As seen in Fig. 8b, when the friction test starts, all the friction coefficient curves of untextured steel under different loads show a dramatically increasing tendency and go through high fluctuations during the whole sliding test, which might result in sever wear of tribo-pairs. Furthermore, the fluctuation intensity of friction coefficient of untextured steel increase with the increase of applied loads.There was no doubt such poor stability of friction coefficient curves would have a negative effect on the working performance and wear resistance of the working parts.

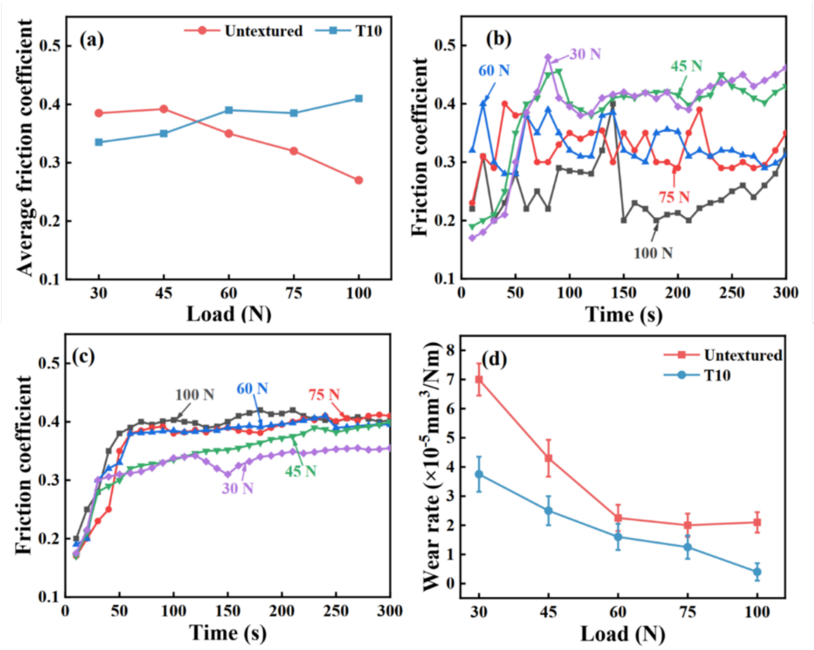

Fig. 8. The friction coefficients and wear rate of untextured surface and T10 texture under high load: (a) average friction coefficient curves, the corresponding friction curves of (b) untextured disk and (c) T10, (d) the corresponding wear rate.

The friction coefficient curves of T10 textured steel under different loads all show the similar tendency, increasing in the running-in stage within the first 30 s and then coming to its steady stage. Nevertheless, compared with untextured S07 steel, the friction coefficient curves are T10 texture much more stable. Thus, it can be obtained that manufacturing texture dimples on S07 steel is effective in improving its stability in friction behavior under high loads.

Fig. 8d shows the wear rate of untextured and textured steels under different pressures. It is obviously that the T10 steel exhibits better wear resistance than untextured steel when the applied load ranges from 30 N to 100 N. The wear rate of untextured steel under 30 N is 6.97×10^{-5} mm^3/Nm, while the value of textured steel under the same pressure is 3.69×10^{-5} mm^3/Nm. Furthermore, both untextured and textured surfaces show a decreasing tendency of wear rate with the increase of applied load, and the wear rate of T10 textured steel is always lower than that of untextured steel under the same load.

The above analyses demonstrate that the T10 textured surface can not decrease average friction coefficient under high loads, but the stability of friction coefficients are greatly enhanced and wear rate is decreased significantly.

To further understand the tribological properties of T10 texture, more tribological experiments under different conditions were conducted. The average friction coefficients and the corresponding friction coefficient curves of T10 under different frequencies are shown in Figure 9a and b. As frequencies increase, the average friction coefficients increase and reach the largest value at 3 Hz and then decrease slightly. The corresponding friction coefficient curves presented in Fig. 9b are stable. The results of the tribological experiments under different loads are shown in Fig. 9c and d. The average friction coefficient shown in Fig. 9c indicates that the average friction coefficients fluctuate as loads increase. The corresponding friction coefficient curves in Fig. 9d are stable.

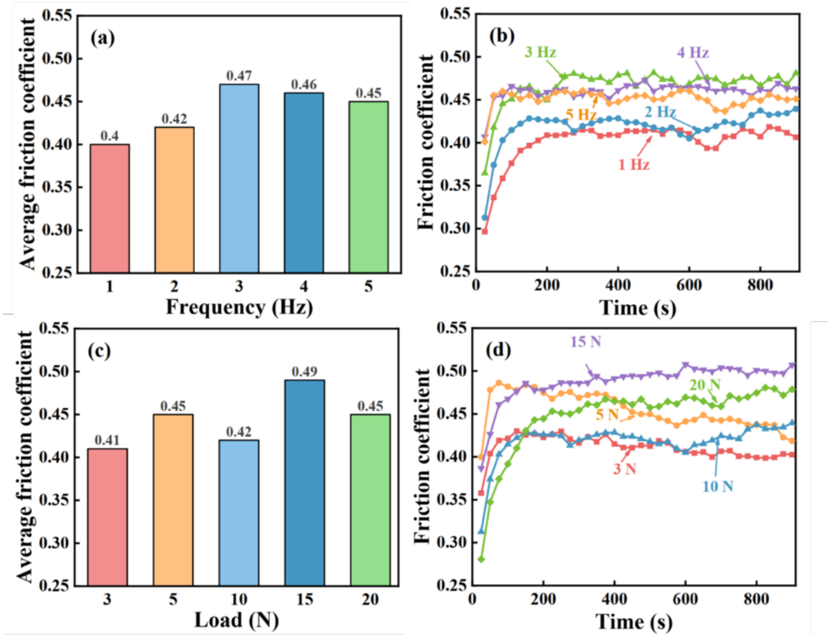

Fig. 9. The average friction coefficients and the corresponding friction coefficient curves of T10 under (a-b) different frequencies and (c-d) loads.

The wear tracks of untextured steel and T10 texture after friction tests are analyzed and the analysis results are showed in Figure 10. As seen in Fig. 10a, parallel grooves could be observed on the wear track of untextured steel surface. As seen in Fig. 10c, there were some parallel grooves on the wear track of textured steel surface. Moreover, there are some materials filled in textured dimples.

In order to further investigate the lubrication mechanism, the wear track surfaces of both steels were analyzed by EDS spectra, and the analysis results are presented in Fig. 10b and d. As seen in Fig. 10b, C, O, Fe and Cu elements could be detected on the wear track of untextured steel, and the detection of Cu elements indicated that the tribo-film might be attributed to the Cu/graphite composite. The EDS analysis results of textured steel was illustrated in Fig. 10d, C, O, Fe and Cu elements are also detected, which also indicates that the tribo-film near the texture sample is attributed to the mating Cu/graphite composite. It is known that the Cu and graphite are both commonly used solid lubrication materials, which can form a transfer film composited of Cu/graphite, improving the friction performance of both steels.

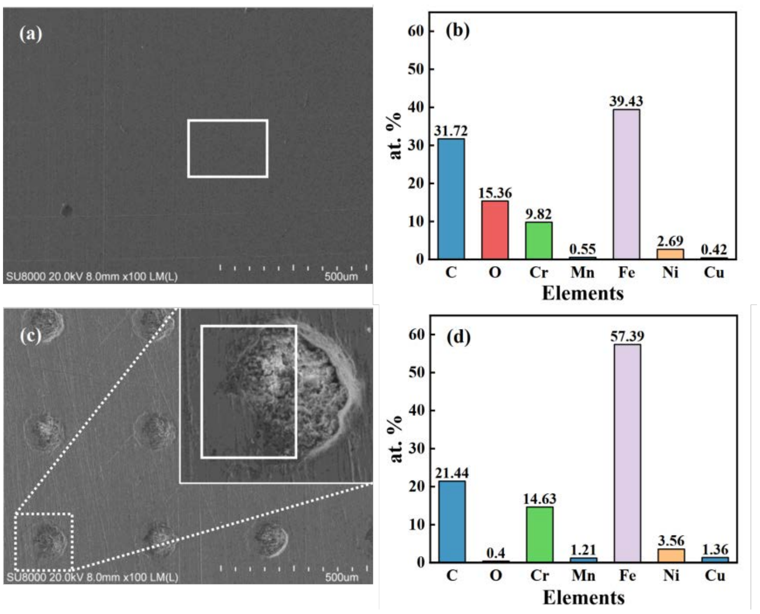

Fig. 10. The SEM images of wear scars and EDS results of (a-b) untextured S07 steel and (c-d) T10

texture.

To further investigate the wear mechanism, the surface morphologies of Cu/graphite pins after tribological test were analyzed by SEM, and the obtained SEM images are showed in Figure 11. As seen in Fig. 11a, the wear surface of Cu/graphite pin after sliding against untextured steel exhibits obvious grooves and delamination, indicating the main wear mechanism is mechanical wear and adhesive wear. Furthermore, the serious adhesive wear might be responsible for the unsteady friction behavior of untextured steel under high applied pressure. In comparison, as seen in Fig. 11b, the wear scar of Cu/graphite pin sliding against textured steel is relatively flat with less parallel grooves and delamination, indicating manufacturing texture dimple is effective in improving the lubricating effect and hindering the mechanical wear and adhesive wear.

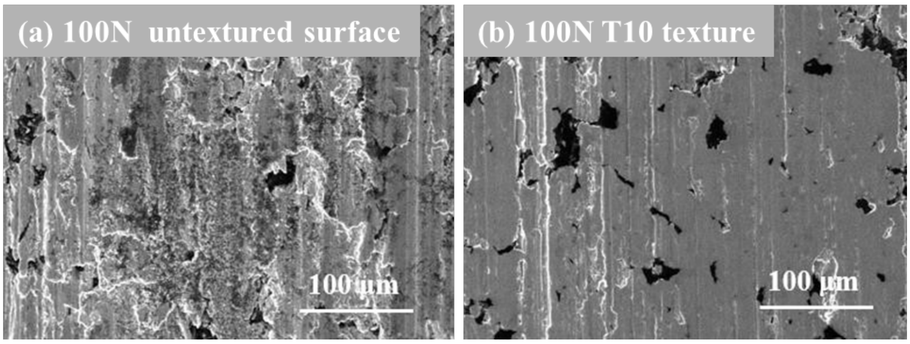

Fig. 11. The wear morphologies of Cu/graphite pin after tribological test: (a) untextured surface, (b) T10 texture.

The tribological mechanism of the textured surface

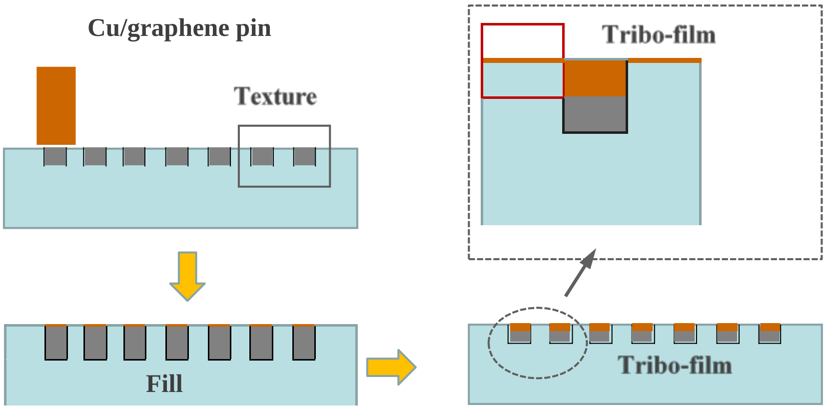

Fig. 12. The tribological mechanism of the textured surface.

The above results show that the textured surface can decrease the friction coefficient and wear rate and enhance the stability of the friction behavior. According to the SEM and EDS results, the tribological mechanism of the textured surface is showed in Figure 12 and explained as follows. Softer than S07 steel disk, Cu/graphene composite pin is easy to wear and exfoliate, which can also fill in the texture dimples. During the exfoliation and filling process, the Cu/graphene composite can fill the micro-pits on the surface and form a soft tribo-film, which may be beneficial to the reduction of friction and decrease of wear.

CONCLUSION

The circle-shaped texture dimple of different area ratios was manufactured on S07 steel surface, and the corresponding diameter and depth were about 100 μm and 26 μm, respectively. The friction behaviors of the untextured and textured surface with different area ratio were investigated and the results showed that T10 texture was most efficient in friction reduction. The tribological performance in water environment was investigated systematically by a pin-on-disk tribometer under different conditions. The results are summarized as following:

(1). The experimental results showed that T10 texture can decrease the friction coefficient under room temperature and 70 ℃. Moreover, under high loads, the average friction coefficients of T10 texture were higher that these of untextured surface, but the friction coefficient curves were much more stable, and the wear rates decreased significantly. The experiments under different frequencies and loads showed that the friction coefficients of T10 texture increased as the frequencies increased while friction coefficients fluctuated as loads increased.

(2). The wear tracks showed that there were sever adhere wear occur to the untextured surface, which might account for the fluctuation of friction coefficient. As for T10 texture, Cu/graphene composite were found in the texture dimples, which could form a Cu/graphene tribo-film on the S07 steel surface, leading to the good anti-friction and anti-wear properties.

(3). Circle-shaped texture dimple was effective in improving the friction behavior and wear resistance of sealing tribo-pairs. Furthermore, the laser texturing process has great potential in improving the tribological performance of contact mechanical seal of turbopump as well as the working performance and service time in the future.

ACKNOWLEDGEMENT

This work was supported by Wear Morphology Analysis and Performance Analysis of Friction Pairs (Grant No. J20151111), and we would like to acknowledge them for their financial support.

REFERENCES

Bai, S., Peng, X., Li, Y., and Sheng, S., "A hydrodynamic laser surface-textured gas mechanical face seal", Tribology Letters, Vol. 38, No. 2, pp. 187-194 (2010).

Bullen, G.N., "Advanced materials for aerospace and space applications", SAE International Journal of Aerospace, Vol. 7, No. 1, pp. 146-155 (2014).

Brunetière, N., and Tournerie, B., "Numerical analysis of a surface-textured mechanical seal operating in mixed lubrication regime", Tribology International, Vol.49, No. 11, pp. 80-89 (2012).

Etsion, I., and Halperin, G., "A laser surface textured hydrostatic mechanical seal", Tribology International, Vol. 45, No.3, pp. 430-434 (2002).

He, Y., Yan, Y. D., Geng, Y. Q., and Brousseau, E., "Fabrication of periodic nanostructures using dynamic plowing lithography with the tip of an atomic force microscope", Applied Surface Science, Vol. 427, pp. 1076-1083 (2018).

Johnson, M.T., Childers, A.S., Ramírez -Rico, J., Wang, H., and Faber, K.T., "Thermal conductivity of wood-derived graphite and copper–graphite composites produced via electrodeposition," Composites Part A: Applied Science and Manufacturing, Vol. 53, pp. 182-189 (2013).

Kusinski, J., Kac, S., Kopia, A., Radziszewska, A., Rozmus-Górnikowska, M., Major, B., Major, L., Marczak, J., and Lisiecki, A., "Laser modification of the materials surface layer-a review paper", Bulletin of the Polish Academy of Sciences: Technical Sciences, Vol. 60, No. 4, pp. 711-728 (2012).

Lu, H., Zhang, P., Ren, S., Guo, J., and Li, X., "The preparation of polytrifluorochloroethylene (PCTFE) micro-particles and application on treating bearing steel surfaces to improve the lubrication effect for copper-graphite (Cu/C)", Applied Surface Science, Vol. 427, pp. 1242-1247 (2018).

Li, J., Liu, S., Yu, A., and Xiang, S., "Effect of laser surface texture on CuSn6 bronze sliding against PTFE material under dry friction", Tribology International, Vol. 118, pp. 37-45 (2018).

Li, X., Li, J., Q., and Dong, G., N., "Bioinspired Topological Surface for Directional Oil Lubrication", ACS Applied Materials & Interfacs, Vol. 12, No. 4, pp. 5113-5119 (2020).

Ma, Q., Zhou, F., Wang, Q., Wu, Z., Chen, K., Zhou, Z., and Li, L.K.Y., "Influence of CrB2 target current on the microstructure, mechanical and tribological properties of Cr-B-C-N coatings in water", RSC Advances, Vol. 6, No. 53, pp. 47698-47711 (2016).

Palerm, S., Bonhomme, C., Guelou, Y., Chopinet, J.N., and Danous, P., "The future of cryogenic propulsion", Acta Astronaut, Vol. 112, pp. 166-173(2015).

Qiu, Y., and Khonsari, M.M., "Experimental investigation of tribological performance of laser textured stainless steel rings", Tribology International, Vol. 44, No. 5, pp. 635-644 (2011).

Silva, L.R.R.D., and Costa, H.L., "Tribological behavior of gray cast iron textured by maskless electrochemical texturing", Wear, Vol. 376, pp. 1601-1610 (2017).

Wang, X., Kato, K., Adachi, K., and Aizawa, K., "Loads carrying capacity map for the surface texture design of SiC thrust bearing sliding in water", Tribology International, Vol. 36, pp. 189-197 (2003).

Wang, J., Jia, Q., Yuan, X., and Wang, S., "Experimental study on friction and wear behaviour of amorphous carbon coatings for mechanical seals in cryogenic environment", Applied Surface Science, Vol. 258, No. 6, pp. 9531-9535 (2012).

Wang, J., Jia, Q., Yuan, X., and Wang, S., "Experimental study on friction and wear behaviour of amorphous carbon coatings for mechanical seals in cryogenic environment", Applied Surface Science, Vol. 258, No. 24, pp. 9531-9535 (2012).

Zhang, G.Y., Yuan, X.Y., Dong, G.N., "The tribological behavior of Ni-Cu-Ag-based PVD coatings for hybrid bearings under different lubrication conditions", Tribology International, Vol. 43, No. 1, pp. 197-201 (2010).

Zhang, G.Y., Zhao, W.G., Yan, X.T., and Yuan, X.Y., "A theoretical and experimental study on characteristics of water-lubricated double spiral–grooved seals", Tribology Transactions, Vol. 54, No. 3, pp. 362-369 (2011).

Zhang, H., Zhang, D.Y., Hua, M., Dong, G.N., and Chin, K.S., "A Study on the Tribological behavior of surface texturing on babbitt alloy under mixed or starved lubrication", Tribology Letters, Vol.56, No.2, pp. 305-315 (2014).

Zhang, H., Hua, M., Dong, G.N., Zhang, D.Y., and Chin, K.S., "A mixed lubrication model for studying tribological behaviors of surface texturing", Tribology International, Vol.93, pp. 583-592 (2016).

Zhang, D., Zhao, F., Li, Y., Li, P., Zeng, Q., and Dong, G., "Study on tribological properties of multi-layer surface texture on Babbitt alloys surface," Applied Surface Science, Vol.390, pp.540-549 (2016).

Zhang, G., Chen, G., Zhao, W., Yan, X., and Zhang, Y., "An experimental test on a cryogenic high-speed hydrodynamic non-contact mechanical seal", Tribology Letters, Vol. 65, No. 3 (2017).

納秒激光表面織構提高機械密封在水環境中的摩擦學性能

趙偉剛
西北工業大學

劉奇 袁恒迪 李毅紅 董光能
西安交通大學

摘 要

液體火箭發動機渦輪泵用機械密封在運行過程中經常發生嚴重的磨損和摩擦振動。本文提出在S07 鋼表面制備有效的圓形織構，並對其表面形貌、力學性能和摩擦學性能進行了系統研究。爲了模擬渦輪泵密封液體的低粘度，在水環境中進行了摩擦學試驗。根據不同面積比織構的實驗結果表明，面積比爲 10%（T10）的織構效率最高。在不同溫度、頻率和載荷下進行了更多的摩擦學實驗，結果表明，T10 織構表面可以降低摩擦系數，提高摩擦系數的穩定性，降低磨損率。此外，根據磨損軌迹的 SEM 和 EDS 分析了織構的摩擦學機理。軟銅/石墨烯複合材料可以填充織構凹陷，在表面形成摩擦膜，有助于減少摩擦磨損。